Geochemical Perspectives Letters

How long for plastics to decompose in the deep sea?

X. Zhang[1,2], X. Peng[1*]

OPEN ACCESS

https://doi.org/10.7185/geochemlet.2222

Abstract

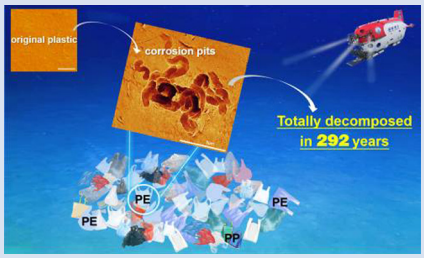

The deep sea floor is recognised as one of the most important final destinations for plastic debris. It is not clear whether the plastic debris in the deep sea could be degraded. Likewise, little is known about how long plastics might last at the deep sea floor. A total of 103 plastic debris were recovered using the manned submersible "*Shenhaiyongshi*" on the deep sea floor (746–3997 m) of the South China Sea (SCS). We found that abundant corrosion structures were present on the surface of polyethylene (PE), which was the dominant type of plastic sample (80 %). The rod-like, filamentous and peanut-like morphologies of the corrosion structures are well in line with those of microorganisms, suggesting that they were derived from biodegradation. The calculation of volume loss of corroded PE showed that about 1.08–13.72 % PE were degraded. Assuming that the most degraded plastic reached the deep sea floor 40 years ago, these plastics will require about 292 years to be totally degraded. Our results provide unique insights into the fate of deep sea plastics and answer the unsolved question about how long plastics may persist in deep sea.

Received 13 April 2022 | Accepted 2 June 2022 | Published 27 June 2022

Introduction

Marine plastic pollution is a major environmental problem affecting human health and ocean ecosystems (Lebreton *et al.*, 2017). It has been estimated that around 15 million metric tons of plastic debris reach the oceans annually (Jambeck *et al.*, 2015), of which 70 % will sink to seafloor (Thompson *et al.*, 2004) and are eventually transported to the deep sea floor (Bergmann *et al.*, 2017; Zhong and Peng, 2021). Complexity and high costs of sampling in the deep sea environments lead to limited recognition of deep sea plastics and restrict understanding of their final fate, although a few studies show that plastic might be ubiquitous at the deep sea floor (Peng *et al.*, 2018, 2019; Nakajima *et al.*, 2021).

It is generally considered that most plastics are quite recalcitrant to degradation and may persist several hundred years or even longer (Chamas *et al.*, 2020), although so far there is no available data on the actual retention times of plastics in various natural environments (Ter Halle *et al.*, 2017; Turner *et al.*, 2020). The degradation of plastic litter in ocean surfaces and beaches, including photo-oxidative, thermal, mechanical, and biodegradation are well recorded (Corcoran *et al.*, 2009; Masry *et al.*, 2021), but it has never been reported in the deep sea where the environment differs from that of the shallow water because of the relatively low temperature, absence of UV light and depleted oxygen (Chamas *et al.*, 2021). Those factors in deep sea environments can inhibit the thermal and photo-oxidative degradation of plastic litter (Nakajima *et al.*, 2021). Consequently, biodegradation might be the most important form of plastic degradation in deep sea. Previous studies showed that the surface of deep sea plastics could supply additional habitats and relevant sources of carbon for colonisation of microbes, along with potentially evolving microorganisms that can degrade plastics (Wright *et al.*, 2020; Wang *et al.*, 2021). However, it still remains unknown whether the deep sea plastics could be degraded by microbes and how long the plastics can persist in deep sea.

Characterisation of Plastics in the Deep Sea

A total of 103 pieces of plastics (Fig. S-1) were recovered from the deep sea floor (746–3997 m) of the northern South China Sea (SCS) using manipulators during 22 dives with the manned submersible *Shenhaiyongshi* (Table S-1, Fig. 1). According to the Raman spectrum (Fig. S-2), the most abundant samples were identified as PE (80 %) and PP (14 %), followed by polyethylene terephthalate (PET, 2 %), polyvinyl chloride (PVC, 2 %), polystyrene (PS, 1 %) and polyesters (Pe, 1 %). Detailed information of plastic samples is listed in Table S-2. Different compositions of plastic samples were observed to have different morphological features on their surfaces. Most of the PE samples showed characteristics of degradation including crumples, grooves, scratches, flakes, cracks, and irregular pits (Fig. S-3). The degradation of the plastic samples was confirmed on the basis of the occurrence of C=O (1659 cm^{-1}), C-O (1032 cm^{-1}) and O-H (3300-3500 cm^{-1}) bonds by Fourier Transform Infrared (FTIR) analysis (Fig. S-3g) (Bhagwat *et al.*, 2021). In the case of PP (Fig. S-4), surface cracking was apparent in most items from the deep sea, also typically observed in the PP collected from the coastal and offshore environment (Rizzo *et al.*, 2021). Degradation *via* crack formation is considered the common degraded pattern of PP, which is possibly

1. Laboratory of Deep-Sea Geology and Geochemistry, Institute of Deep-Sea Science and Engineering, Chinese Academy of Sciences, Sanya, 572000, China
2. University of Chinese Academy of Sciences, Chinese Academy of Sciences, Beijing, 100049, China
* Corresponding author (email: xtpeng@idsse.ac.cn)

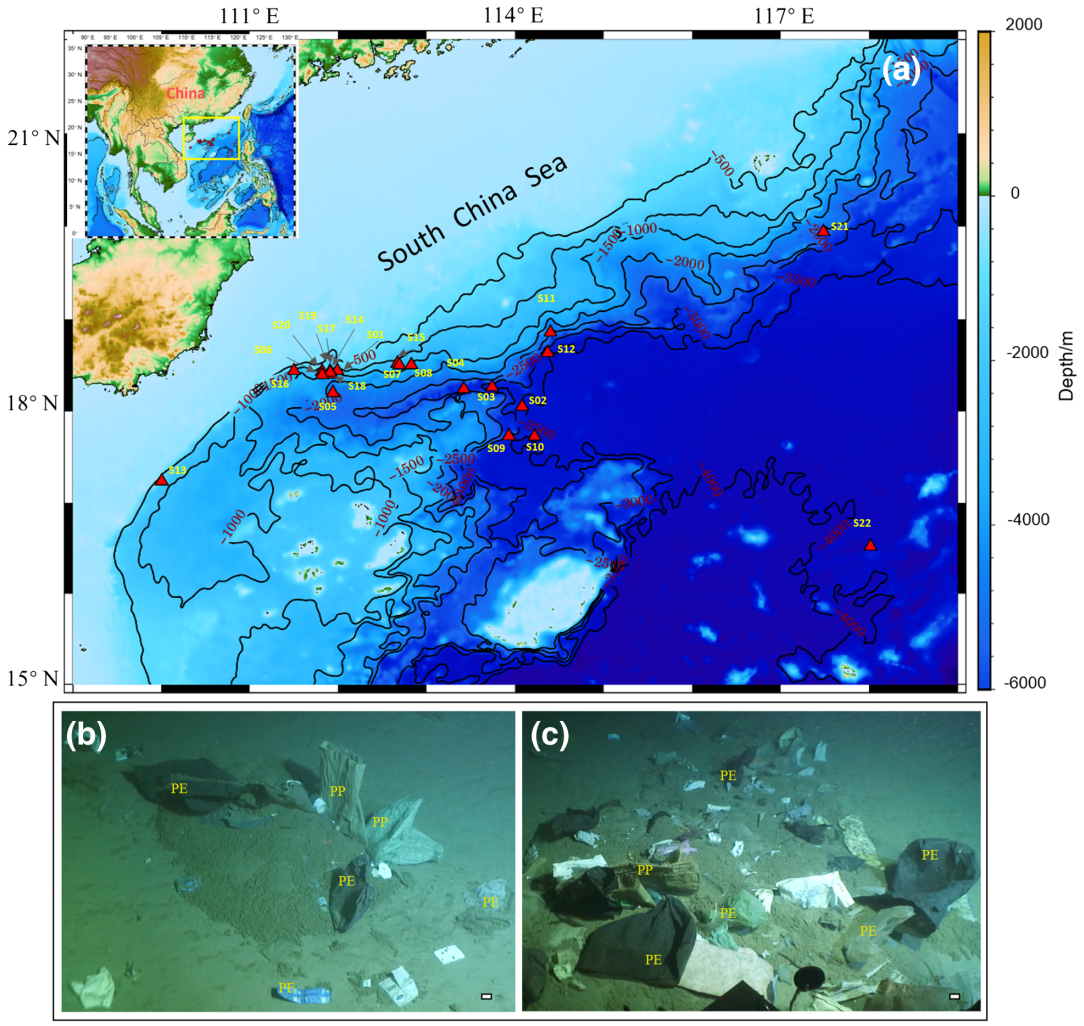

Figure 1 **(a)** Sampling sites of plastic litter in the northern South China Sea (Table S-1 lists detailed information of sampling locations; red triangles refer to the sampling sites). **(b)** Plastic bags, woven bags, and packing bags accumulated on the seafloor of site S06. **(c)** Various types of plastics with different colours accumulated on the seafloor of site S14. PE: polyethylene, PP: polypropylene, scale bar = 10 cm.

caused by photo-oxidation when they were in shallow water (Song *et al.*, 2017; Tang *et al.*, 2019). While other plastics, such as PET, PS, PVC and Pe (Fig. S-5), exhibited rather smooth surfaces with only visible physical scratches.

Degradation on the Surface of PE

Especially intriguing were numerous corrosion pits found on the surface of eighteen PE debris (Fig. 2a–g). The plastic surface showed a high degree of degradation, which was pockmarked with abundant pits linked to each other (Fig. 2a,b). Two structures of corrosion pits, including short rod-like and peanut-like structures, were distributed and overlapped on the surface of plastics (Fig. 2c,d). In addition, other forms of pits were also observed on PE surfaces, such as worm-like and filamentous structures (Fig. 2e–g). All pits are 1-2 μm in length and their morphologies just coincide with those of some bacteria.

The three dimensional morphology by photo-induced force microscopy (PiFM) showed the typical worm-like structures (Fig. 3a,b). The Ra (Roughness Average) value is usually used to indicate surface roughness. It is evident that the more heavily degraded plastic exhibits higher roughness. PiFM can be used to probe the micron scale topography of pits to higher accuracy and precision in the vertical dimension compared to the Scanning Electron Microscope (SEM). Through the cross sectional analysis of PiFM images, the worm-like pits are approximately 0.9 μm in width (0.45 × 2 μm) and 144.3–289.8 nm in depth in the relatively early stages of degradation (Fig. 3c). As degradation progresses, the pit depths become deeper, up to about 572.2–663.2 nm deep (Fig. 3d).

A peak at 1035 cm^{-1} in PiFM spectrum was distinctly identified on the surface of pits, attributed to -C-O- bond stretching characteristic of ethers, carboxylic acids and esters (Andrady *et al.*, 2022). This feature of spectra was consistent with those from laboratory experiments of microbial degradation (Puglisi *et al.*, 2019; Khandare *et al.*, 2021). In addition, the corrosion pits found in this study highly resemble those from previous laboratory experiments which show similar corrosion pits are produced by microbes during biodegradation of plastics (Yoshida *et al.*, 2016; Puglisi *et al.*, 2019), further suggesting a biological origin. Furthermore, surfaces of PE stained using SYBR green I showed that rod-like cells were densely present on the surface of pits (Fig. S-7a,b), together with the objects with microbial morphologies observed by SEM (Fig. 2h), also corroborating evidence suggesting that the formation of corrosion pits is potentially caused by microbial degradation.

Only a few studies on the surface characteristics of plastics sinking into the deep sea naturally have been performed due to

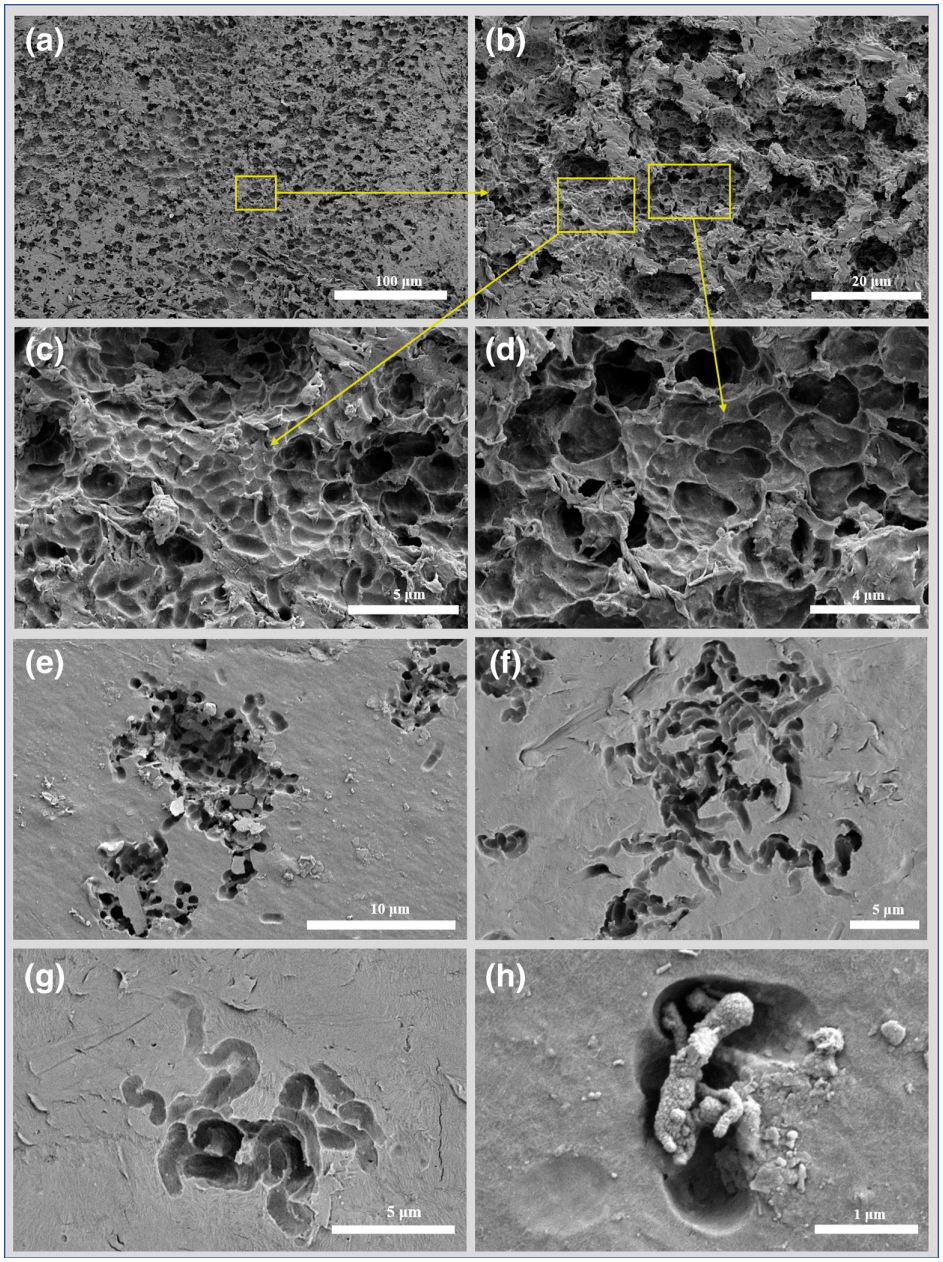

Figure 2 Typical examples of SEM images of PE samples with corrosion pits. (a) SEM photomicrographs of partial surface of P102. **(b)** Enlarged image of the yellow line marked area in a. **(c, d)** Enlarged image of the yellow line marked area in **b**. **(e, f, g)** SEM images of different corrosion pits observed on the surface of P27, P19 and P18. **(h)** Objects with microbial morphologies on the surface of pits of P103.

sampling difficulties. Krause *et al.* (2020) found only two bulk plastic bags of PE at a water depth of 4150 m during the ROV dives. Nevertheless, the two items showed no apparent sign of biological degradation, possibly due to the short residence time after they reached the seafloor. While in our study, the unique pits suggestive of a biodegradation activity were found for the first time on the surface of plastics on the deep sea floor. This suggests that microbial degradation could happen more easily than chemical degradation in extreme conditions of the deep ocean that is characterised by lower temperatures, absence of UV light and lower oxygen concentration than in the shallow sea, although the biodegradation speed of plastics in deep sea is relatively low. Currently, the roles of enzymes in plastic biodegradation have been highlighted in several studies, including microbial depolymerases, hydrolases, lipases, and peroxidases (Roohi *et al.*, 2017; Amobonye *et al.*, 2021). Widely present pits on the surface of PE may also suggest that cold-adapted enzymes produced by barophilic/tolerant microorganisms and psychrophiles possibly play important roles in degrading plastics in the deep sea (Urbanek *et al.*, 2018; Atanasova *et al.*, 2021).

Quantification of Degradation of PE

We used the volume loss to quantify the degradation of PE plastics at the deep sea floor. According to SEM images of cross sections (Fig. 4a–d), the thicknesses of the eighteen PE samples with corrosion pits in our study ranged from 13.236–28.467 µm. The pit density and the depth, mouth area, volume of individual pits were analysed from the PiFM images. The statistical results are tabulated in Table S-3. As shown in Figures 4e and S-6, all the pits at least 1 µm wide and 0.1 µm deep on the surface of P102 were counted and the depths of these pits were analysed by SurfaceWorks (Molecular Vista, Inc.). The statistical results showed that the

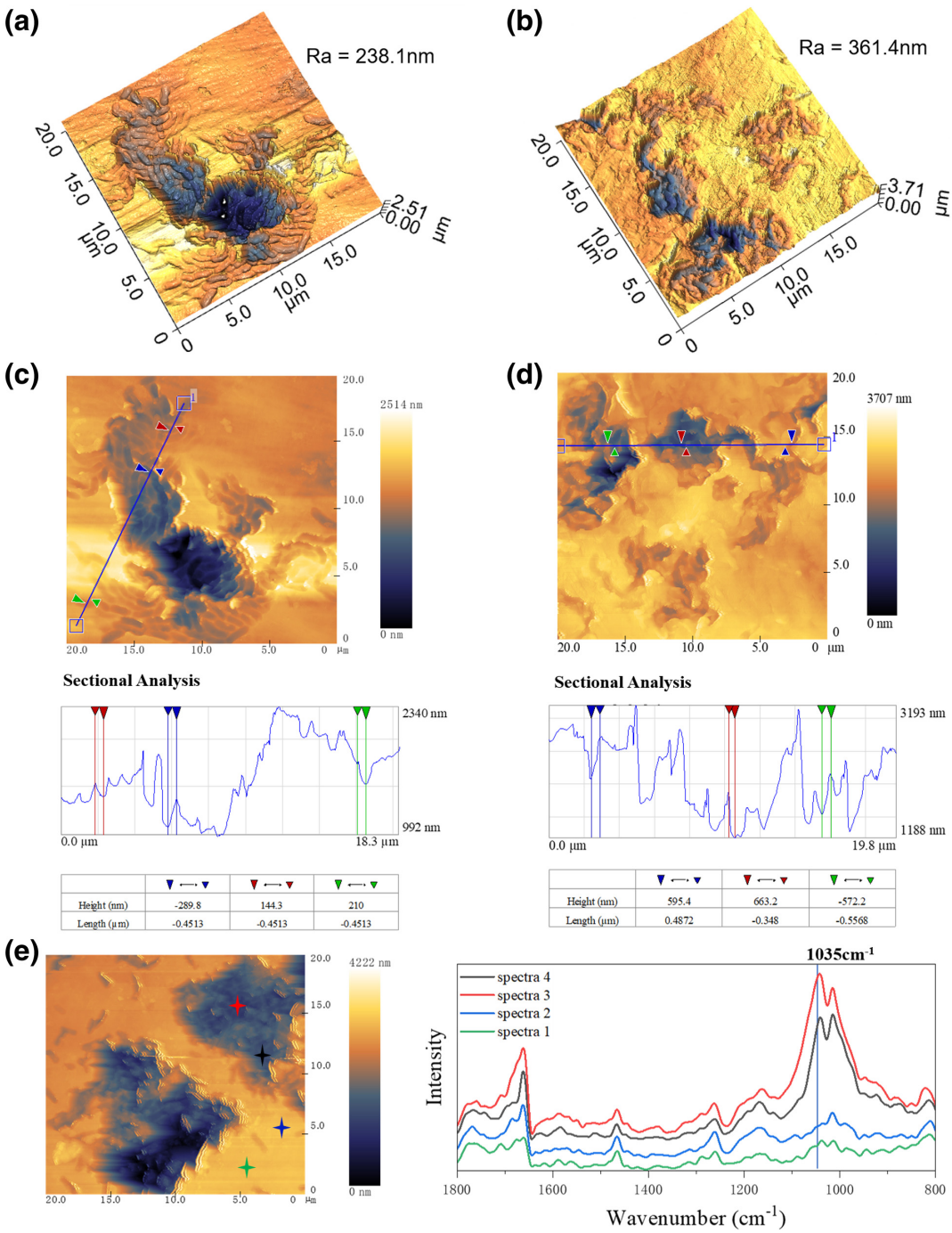

Figure 3 Typical examples of PiFM images, spectra, and sectional analysis of PE with corrosion pits. (a, b) 3D images of worm-like structures. Ra represents roughness average. **(c, d)** 2D images and the cross sectional analysis along the line. **(e)** PiFM images and spectra corresponding to inside of corrosion pits (spectra 3, 4) and outside of pits (spectra 1, 2).

depth, mouth area, and volume of corrosion pits on the surface of plastic (P102) are 1.733 μm, 24.11 μm^2, 35.67 μm^3 respectively (Fig. 4f–h). Using the calculated volume ratio of corroded pits and plastics, we could estimate that about 1.08–13.72 % of a piece of polyethylene plastic on the deep sea floor might be degraded.

So far, there are no appropriate ways to date large plastics that are deposited into the oceans because these materials have only been manufactured over a relatively short period of time (several decades) and there is a lack of sedimentary sequences (Turner *et al.*, 2020). Some studies about plastic persistence and deposition ages of plastic show they are, according to the outer packing, from a distinct temporal source (Ioakeimidis *et al.*, 2016; Krause *et al.*, 2020). However, there is no information available on the date of manufacture of our plastic samples. In order to constrain the deposition ages of plastics, we use the dating data of microplastic pollution in the same research area of the South China Sea, which show microplastic pollution in this area commenced in the 1980s and has a forty year pollution history (Chen *et al.*, 2020). Assuming that the most degraded plastics in our samples have already been at the deep sea floor for 40 years, it would take about 292 years for these plastics to be fully degraded. This result provides the upper limitation for the degradation time of PE in deep sea and represents the maximum degradation time for these deep sea plastics.

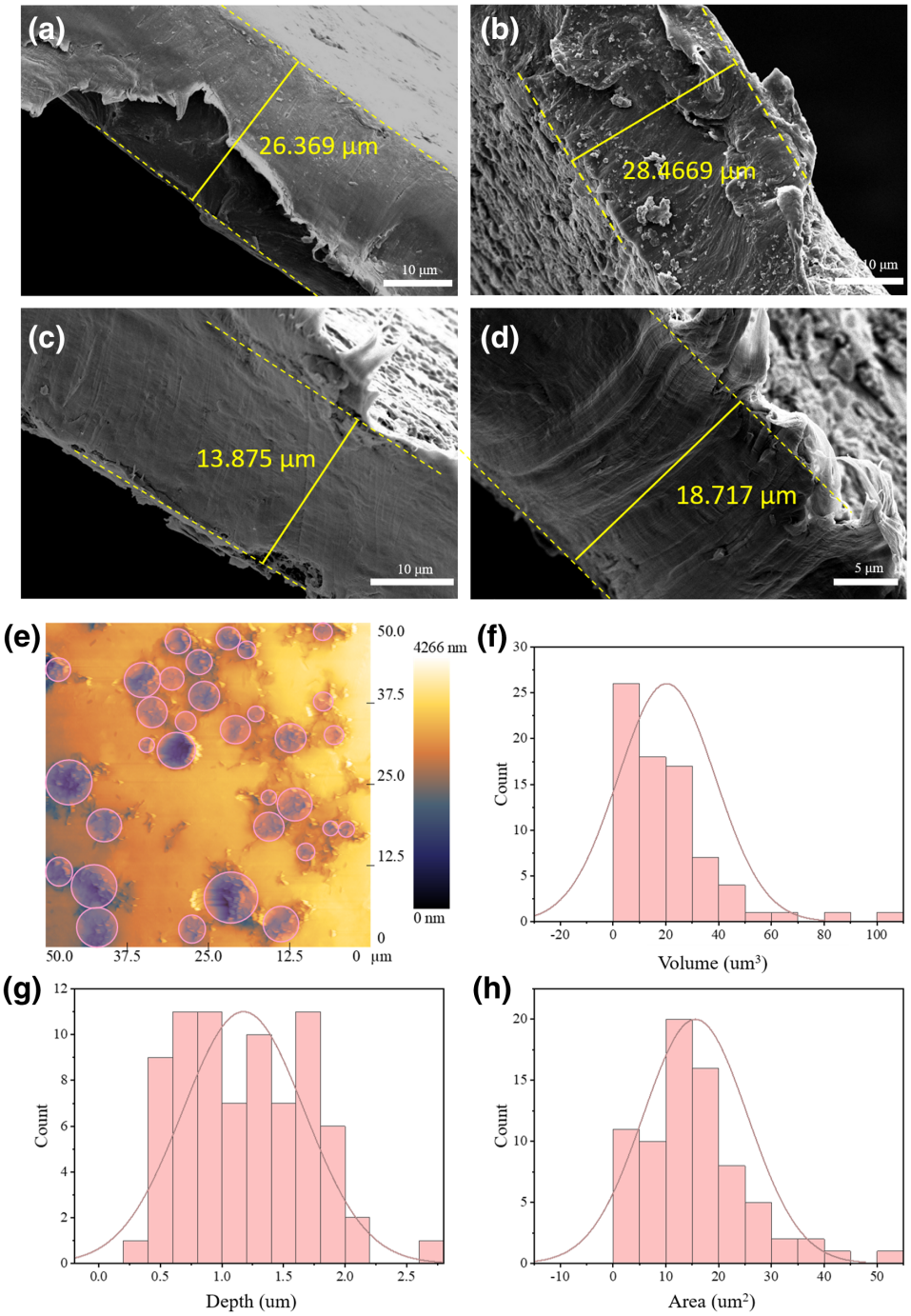

Figure 4 **(a, b, c, d)** Examples of SEM images of thickness of PE samples with corrosion pits. **(e)** PiFM image of P102. The circles in red were pits at least 1 µm wide and 0.1 µm deep. **(f, g, h)** Histogram of the depth, area and volume of corrosion pits of P102 measured by PiFM.

Conclusions and Implications

The fate of plastics in marine environments is a matter that is still in debate. Some have argued that all the conventional plastics entering oceans have never been degraded and still remain either as whole items or as fragments to date (Barnes *et al.*, 2009). This study provides the first evidence that plastics in the deep sea can be degraded, and estimates that the maximum residence time of PE is about 292 years, although there exist some uncertainties regarding the dating of plastics. In addition, the mere presence of corrosion pits on PE suggests other types of plastics, such as PP, PET, PVC and PS, will persist on the deep sea floor for a far longer period of time, and could have more profound and lasting threats to the deep sea ecosystem. Strict control measures should be taken to prevent these refractory plastics from entering the oceans.

Acknowledgements

We thank the crews and scientists of R/V *Tansuoyihao* and pilots of HOV *Shenghaiyongshi* in the voyages (TS07, TS12, TS16, TS2-1-3). This work was supported by National Key Research and Development Plan of China (2016YFC0302301).

Editor: Eric H. Oelkers

Additional Information

Supplementary Information accompanies this letter at https://www.geochemicalperspectivesletters.org/article2222.

Cite this letter as: Zhang, X., Peng, X. (2022) How long for plastics to decompose in the deep sea?. *Geochem. Persp. Let.* 22, 20–25. https://doi.org/10.7185/geochemlet.2222

References

Amobonye, A., Bhagwat, P., Singh, S., Pillai, S. (2021) Plastic biodegradation: Frontline microbes and their enzymes. *Science of The Total Environment* 759, 143536. https://doi.org/10.1016/j.scitotenv.2020.143536

Andrady, A.L., Law, K.L., Donohue, J., Koongolla, B. (2022) Accelerated degradation of low-density polyethylene in air and in sea water. *Science of The Total Environment* 811, 151368. https://doi.org/10.1016/j.scitotenv.2021.151368

Atanasova, N., Stoitsova, S., Paunova-Krasteva, T., Kambourova, M. (2021). Plastic degradation by extremophilic bacteria. *International Journal of Molecular Sciences* 22, 5610. https://doi.org/10.3390/ijms22115610

Barnes, D.K., Galgani, F., Thompson, R.C., Barlaz, M. (2009) Accumulation and fragmentation of plastic debris in global environments. *Philosophical Transactions of the Royal Society B: Biological Sciences* 364, 1985–1998. https://doi.org/10.1098/rstb.2008.0205

Bergmann, M., Wirzberger, V., Krumpen, T., Lorenz, C., Primpke, S., Tekman, M.B., Gerdts, G. (2017) High quantities of microplastic in Arctic deep-sea sediments from the HAUSGARTEN observatory. *Environmental Science & Technology* 51, 11000–11010. https://doi.org/10.1021/acs.est.7b03331

Bhagwat, G., Carbery, M., Anh Tran, T.K., Grainge, I., O'Connor, W., Palanisami, T. (2021) Fingerprinting Plastic-Associated Inorganic and Organic Matter on Plastic Aged in the Marine Environment for a Decade. *Environmental Science & Technology* 55, 7407–7417. https://doi.org/10.1021/acs.est.1c00262

Chamas, A., Moon, H., Zheng, J., Qiu, Y., Tabassum, T., Jang, J.H., Abu-Omar, M., Scott, S.L., Suh, S. (2020) Degradation rates of plastics in the environment. *ACS Sustainable Chemistry & Engineering* 8, 3494–3511. https://doi.org/10.1021/acssuschemeng.9b06635

Chen, M., Du, M., Jin, A., Chen, S., Dasgupta, S., Li, J., Xu, H., Ta, K., Peng, X. (2020) Forty-year pollution history of microplastics in the largest marginal sea of the western Pacific. *Geochemical Perspectives Letters* 13, 42–47. https://doi.org/10.7185/geochemlet.2012

Corcoran, P.L., Biesinger, M.C., Grifi, M. (2009) Plastics and beaches: a degrading relationship. *Marine Pollution Bulletin* 58, 80–84. https://doi.org/10.1016/j.marpolbul.2008.08.022

Ioakeimidis, C., Fotopoulou, K.N., Karapanagioti, H.K., Geraga, M., Zeri, C., Papathanassiou, E., Galgani, F., Papatheodorou, G. (2016) The degradation potential of PET bottles in the marine environment: An ATR-FTIR based approach. *Scientific Reports* 6, 1–8. https://doi.org/10.1038/srep23501

Jambeck, J.R., Geyer, R., Wilcox, C., Siegler, T.R., Perryman, M., Andrady, A., Narayan, R., Law, K.L. (2015) Plastic waste inputs from land into the ocean. *Science* 347, 768–771. https://doi.org/10.1126/science.1260352

Khandare, S.D., Chaudhary, D.R., Jha, B. (2021) Marine bacterial biodegradation of low-density polyethylene (LDPE) plastic. *Biodegradation* 32, 127–143. https://doi.org/10.1007/s10532-021-09927-0

Krause, S., Molari, M., Gorb, E.V., Gorb, S.N., Kossel, E., Haeckel, M. (2020) Persistence of plastic debris and its colonization by bacterial communities after two decades on the abyssal seafloor. *Scientific Reports* 10, 1–15. https://doi.org/10.1038/s41598-020-66361-7

Lebreton, L., Van Der Zwet, J., Damsteeg, J.W., Slat, B., Andrady, A., Reisser, J. (2017) River plastic emissions to the world's oceans. *Nature Communications* 8, 1–10. https://doi.org/10.1038/ncomms15611

Masry, M., Rossignol, S., Gardette, J.L., Therias, S., Bussière, P.O., Wong-Wah-Chung, P. (2021) Characteristics, fate, and impact of marine plastic debris exposed to sunlight: A review. *Marine Pollution Bulletin* 171, 112701. https://doi.org/10.1016/j.marpolbul.2021.112701

Nakajima, R., Tsuchiya, M., Yabuki, A., Masuda, S., Kitahashi, T., Nagano, Y., Ikuta, T., Isobe, N., Nakata, H., Ritchie, H., Oguri, K., Osafune, S., Kawamura, K., Suzukawa, M., Yamauchi, T., Iijima, K., Yoshida, T., Chiba, S., Fujikura, K. (2021) Massive occurrence of benthic plastic debris at the abyssal seafloor beneath the Kuroshio Extension, the North West Pacific. *Marine Pollution Bulletin* 166, 112188. https://doi.org/10.1016/j.marpolbul.2021.112188

Peng, X., Cheng, M., Chen, S., Dasgupta, S., Xu, H., Ta, K., Du, M., Guo, Z., Bai, S. (2018) Microplastics contaminate the deepest part of the world's ocean. *Geochemical Perspectives Letters* 9, 1–5. https://doi.org/10.7185/geochemlet.1829

Peng, X., Dasgupta, S., Zhong, G., Du, M., Xu, H., Chen, M., Chen, S., Ta, K., Li, J. (2019) Large debris dumps in the northern South China Sea. *Marine Pollution Bulletin* 142, 164–168. https://doi.org/10.1016/j.marpolbul.2019.03.041

Puglisi, E., Romaniello, F., Galletti, S., Boccaleri, E., Frache, A., Cocconcelli, P.S. (2019) Selective bacterial colonization processes on polyethylene waste samples in an abandoned landfill site. *Scientific Reports* 9, 1–13. https://doi.org/10.1038/s41598-019-50740-w

Rizzo, M., Corbau, C., Lane, B., Malkin, S.Y., Bezzi, V., Vaccaro, C., Nardin, W. (2021) Examining the dependence of macroplastic fragmentation on coastal processes (Chesapeake Bay, Maryland). *Marine Pollution Bulletin* 169, 112510. https://doi.org/10.1016/j.marpolbul.2021.112510

Roohi, Bano, K., Kuddus, M., Zaheer, M.R., Zia, Q., Khan, M.F., Gupta, A.Md., Aliev, G. (2017) Microbial enzymatic degradation of biodegradable plastics. *Current Pharmaceutical Biotechnology* 18, 429–440. https://doi.org/10.2174/1389201018666170523165742

Song, Y.K., Hong, S.H., Jang, M., Han, G.M., Jung, S.W., Shim, W.J. (2017) Combined effects of UV exposure duration and mechanical abrasion on microplastic fragmentation by polymer type. *Environmental Science & Technology* 51, 4368–4376. https://doi.org/10.1021/acs.est.6b06155

Tang, C.C., Chen, H.I., Brimblecombe, P., Lee, C.L. (2019) Morphology and chemical properties of polypropylene pellets degraded in simulated terrestrial and marine environments. *Marine Pollution Bulletin* 149, 110626. https://doi.org/10.1016/j.marpolbul.2019.110626

Ter Halle, A., Ladirat, L., Martignac, M., Mingotaud, A.F., Boyron, O., Perez, E. (2017) To what extent are microplastics from the open ocean weathered? *Environmental Pollution* 227, 167–174. https://doi.org/10.1016/j.envpol.2017.04.051

Thompson, R.C., Olsen, Y., Mitchell, R.P., Davis, A., Rowland, S.J., John, A.W., McGonigle, D., Russell, A.E. (2004) Lost at sea: where is all the plastic? *Science* 304, 838. https://doi.org/10.1126/science.1094559

Turner, A., Arnold, R., Williams, T. (2020) Weathering and persistence of plastic in the marine environment: Lessons from LEGO. *Environmental Pollution* 262, 114299. https://doi.org/10.1016/j.envpol.2020.114299

Urbanek, A.K., Rymowicz, W., Mirończuk, A.M. (2018) Degradation of plastics and plastic-degrading bacteria in cold marine habitats. *Applied Microbiology and Biotechnology* 102, 7669–7678. https://doi.org/10.1007/s00253-018-9195-y

Wang, J., Peng, C., Li, H., Zhang, P., Liu, X. (2021) The impact of microplastic-microbe interactions on animal health and biogeochemical cycles: a mini-review. *Science of The Total Environment* 773, 145697. https://doi.org/10.1016/j.scitotenv.2021.145697

Wright, R.J., Erni-Cassola, G., Zadjelovic, V., Latva, M., Christie-Oleza, J.A. (2020) Marine plastic debris: a new surface for microbial colonization. *Environmental Science & Technology* 54, 11657–11672. https://doi.org/10.1021/acs.est.0c02305

Yoshida, S., Hiraga, K., Takehana, T., Taniguchi, I., Yamaji, H., Maeda, Y., Toyohara, K., Miyamoto, K., Kimura, Y., Oda, K. (2016) A bacterium that degrades and assimilates poly (ethylene terephthalate). *Science* 351, 1196–1199. https://doi.org/10.1126/science.aad6359

Zhong, G., Peng, X. (2021) Transport and accumulation of plastic litter in submarine canyons—The role of gravity flows. *Geology* 49, 581–586. https://doi.org/10.1130/G48536.1

Geochemical Perspectives Letters

How long for plastics to decompose in the deep sea?

X. Zhang, X. Peng

Supplementary Information

The Supplementary Information includes:

- Material and Methods
- Tables S-1 to S-3
- Figures S-1 to S-7
- Supplementary Information References

Material and Methods

Sample collection

One hundred and three plastic samples were collected from deep sea floor (746–3997 m depth) of the northern South China Sea (SCS), including continental slope, canyon, trough, seamount and basin geomorphic units, during 22 dives with the manned submersible Shenhaiyongshi. Table S-1 contains details of sampling. After collection, all samples were then stored at −20 °C until further analysis.

Samples treatment

Several pieces of 1 × 1 cm^2 areas of random regions were cut out from the different plastic items with a sterilised pair of scissors for characterisation analysis. All pieces were immersed in 10 % H_2O_2 solution for 5 min and then in an ultrasonic bath for 10 s to remove the visible adherent and biofilms. Subsequently, samples were finally rinsed with sterile water, cleaned in 100 % ethanol, and dried at room temperature.

1 × 1 cm^2 areas were cut out from the different plastic items with a sterilised pair of scissors for cell staining. All pieces were fixed in 4 % paraformaldehyde for 4h, then repeatedly rinsed with sterilised phosphate-buffered saline (PBS), and transferred to a 1:1 ethanol/PBS solution and stored at −20 °C.

Methods and analysis

Raman spectroscopy

The polymer types of plastic samples were identified by a WiTec alpha300 R (WiTec GmbH) confocal Raman imaging system, equipped with a 532 nm Nd:YAG laser and spectrometer with a CCD camera (Peltier cooled to ~60 °C). 50× objective (NA = 0.75) and a Raman range of 62–3866 cm^{-1} were used in our experiments. All samples were excited at a power of 0.200 mW over 5 integration cycles of 10 s duration each.

The Raman spectrum of diagnostic polyethylene (PE) showed peaks near 2882, 2849, 1440, 1295, 1062 and 1128 cm^{-1}, which are characteristic of this polymer (Fig. S-2a). High-density polyethylene (HDPE) was distinguished from low-density polyethylene (LDPE) by the presence of a sharp and strong peak at 1421 cm^{-1}, with its presence indicating

HDPE (Sato *et al*., 2002). In our samples, most polyethylene exhibited a broader peak from 1500 to 2500 cm^{-1} due to excitation of fluorescent impurities (Fig. S-2a,b). However, blue and red PE were only exhibited two weaker peaks around 2882 and 2849 cm^{-1}, which can be attributed to strong fluorescence hindering spectra acquisition (Fig. S-2b) (Lenz *et al*., 2015). Therefore, about 26 % PE in our samples could not be positively distinguished, and was classified as unknown PE. Three additional peaks in Raman spectrum at 141, 445 and 608 cm^{-1} of PE indicated the incorporation of titanium dioxide (TiO2) polymorphs anatase (141 cm^{-1}) and rutile (445, 608 cm^{-1}) (Nauendorf *et al*., 2016). Other polymer composition of our samples, including polypropylene (PP), polystyrene (PS), polyethylene terephthalate (PET), polyvinyl chloride (PVC), and Polyester (Pe) were positively identified based on spectra compared to known standards (Käppler *et al*., 2016).

Scanning electron microscope (SEM)

All pieces of different plastics were dried over night at 25 °C, then fixed on the sample stages using double-sticky carbon plates and sputter-coated with Au for 70 seconds at 20 mA before analysis. The surface morphology of all the collected plastic debris was examined using a Thermo scientific Apreo C scanning electron microscope (SEM) equipped with an Energy-dispersive X-ray spectroscopy and AZtec system provided by Oxford Instruments. The SEM was operated at 2.0 kV electron at a working distance of 10.0 mm accelerating voltage to provide the highest resolution and images were obtained using the secondary electron emission detector.

Fourier Transform Infrared (FTIR)

Surface oxidation of samples were analysed using an attenuated total reflectance ATR-FTIR (IRTracer-100, Shimadzu, Japan). The FTIR spectra were recorded from 400 to 4000 cm^{-1} at a resolution of 4 cm^{-1}.

Photoinduced force microscopy (PiFM)

The photo-induced force microscopy (PiFM) data were collected on a VistaScope-infrared (IR) microscope (Molecular Vista, Inc.). PiFM topographic images of varying sizes (20 and 50 μm), were operated in dynamic contact mode using NCHAu tips from Nanosensors, at 256 x 256 pixels and 512 x 512 pixels resolution, respectively. The IR source used to excite the sample was manufactured from Block Engineering with a wavenumber range of 760–1860 cm^{-1} and a resolution of 4 cm^{-1}.

Quantitative analysis of corrosion pits

Three random regions about 50×50 μm^2 of every piece of plastic samples were selected for PiFM analysis. The number of pits (density of pits) that are at least 1 μm wide and 0.1 μm deep in the scanned images per unit area (50×50 μm) was counted from the PiFM images. Meanwhile, the depth, mouth area, and volume of individual pits were also analysed with the sectional analyses. The statistical results were tabulated in Table S-3. The PiFM data (PiFM micrographs, point spectra, IR images) were processed using SurfaceWorks software (Molecular Vista, Inc.).

Cell staining

SYBR Green I is a highly sensitive fluorescent nucleic acid stain (Briggs and Jones, 2005). SY BR Green I (Solarbio, China) was diluted 100 times with ultrapure water before use. After being fixed, the plastic pieces were covered with SYBR Green I for 10 min at room temperature and then photographed using a fluorescence microscope (Leica DFC 7000T).

Supplementary Tables

Table S-1 List of detailed information of sampling locations.

Site	Dive code	Depth(m)	Longitude(°E)	Latitude (°N)	Dive date	Location	Total sample count
S01	SY082	1732	111.99	18.44	2018/5/28	Xisha Trough	4
S02	SY083	3408	114.08	18.05	2018/5/29	Xisha Trough	2
S03	SY085	3233	113.74	18.26	2018/6/1	Xisha Trough	1
S04	SY086	3103	113.42	18.24	2018/6/2	Xisha Trough	1
S05	SY087	2200	111.94	18.20	2018/6/3	Xisha Trough	2
S06	SY151	1581	111.81	18.43	2019/6/26	Xisha Trough	10
S07	SY152	1200	112.67	18.52	2019/6/27	Xisha Trough	2
S08	SY153	1400	112.82	18.50	2019/6/28	Xisha Trough	1
S09	SY154	3286	113.93	17.73	2019/6/29	Xisha Trough	2
S10	SY155	3515	114.22	17.72	2019/6/30	Xisha Trough	1
S11	SY156	2791	114.40	18.86	2019/7/1	Xisha Trough	9
S12	SY157	3570	114.36	18.63	2019/7/2	Xisha Trough	3
S13	SY158	746	110.00	17.23	2019/7/4	Qiongdongnan Basin	1
S14	SY159	1629	111.90	18.43	2019/7/5	Xisha Trough	3
S15	SY163	1206	112.65	18.50	2019/7/8	Xisha Trough	3
S16	SY164	1246	111.50	18.44	2019/7/9	Xisha Trough	6
S17	SY226	1913	111.91	18.41	2020/3/11	Xisha Trough	2
S18	SY227	1900	111.91	18.40	2020/3/12	Xisha Trough	16
S19	SY228	1833	111.91	18.42	2020/3/13	Xisha Trough	21
S20	SY229	1751	111.82	18.39	2020/3/14	Xisha Trough	5
S21	SY258	2651	117.48	19.94	2020/8/16	Deposition of Dongsha	7
S22	SY269	3997	118.01	16.52	2020/8/26	Seamount of central SCS	1

Table S-2 List of detailed information of plastic samples.

Site	Sample code	Type	Color	Composition	Surface feature
S01	P1	Plastic bag	Blue	PE*	Fractures
	P2	Plastic bag	Black	LDPE	Surface oxidation
	P3	Balloon	Multicolor	PE*	Smooth, surface cracks
	P4	Plastic bag	Black	LDPE	Hilly surface with numerous protrusions
S02	P5	Plastic bag	Black	LDPE	Rough surface
	P6	Rope	White	PP	Surface cracks
S03	P7	Packing	Light blue	LDPE	Smooth, surface cracks
S04	P8	Packing bag	Silver	LDPE	rough surface
S05	P9	Packing bag	Translucent	HDPE	Rough surface filamentous, cracking
S06	P10	Plastic bag	Blue	HDPE	Adhering fibrous particles
	P11	Plastic bag	Black	HDPE	Corrosion pits

	P12	Packing bag	Translucent	LDPE	Corrosion pits
	P13	Packing bag	Translucent	PP	Severe surface cracking
	P14	Water bottle	Translucent	PET	Smooth and scratches
	P15	Plastic bag	Black	HDPE	Uneven surface
	P16	Plastic bag	White	LDPE	Cracks
	P17	Packing bag	Multicolor	LDPE	Rough surface
	P18	Plastic bag	Black	HDPE	Corrosion pits
	P19	Packing bag	Translucent	PE*	Countless corrosion pits of being linked
	P20	Packing bag	Translucent	PE*	Corrosion pits
S07	P21	Packing bag	Silver	LDPE	Uneven surface
	P22	Plastic bag	Translucent	PE*	Smooth, surface cracks
S08	P23	Plastic bag	White	LDPE	rough surface
S09	P24	Plastic bag	White	HDPE	Adhering fibrous particles
	P25	Plastic bag	Translucent	PE*	Irregular fractures
S10	P26	Fiber	Black	Polyester	Smooth
	P27	Packing	Blue	HDPE	Corrosion pits
	P28	Rope	Blue	PP	Severe surface cracking
	P29	Rope	Translucent	PP	Linear cracks
	P30	Packing	Translucent	PS	Smooth
S11	P31	Rope	Mustard	PP	linear cracks
	P32	Rope	Black	PP	linear cracks
	P33	Woven bag	Translucent	PP	Perpendicular and parallel cracks
	P34	Packing bag	Blue and white	LDPE	Wrinkles
	P35	Rope	Yellow	PVC	Smooth, and scratches
	P36	Packing bag	Silver	HDPE	Adhering fibrous particles
S12	P37	Packing bag	Multicolor	LDPE	Rough surface filamentous, cracking
	P38	Plastic bag	White	HDPE	Uneven surface
S13	P39	Plastic bag	White	LDPE	Corrosion pits
	P40	Plastic bag	Blue	PE*	Corrosion pits
S14	P41	Plastic bag	White	HDPE	Adhering fibrous particles
	P42	Woven bag	White	PP	Irregular holes
	P43	Water bottle	Translucent	PET	Smooth and grooves
S15	P44	Packing	Blue	PVC	Smooth and scratches
	P45	Woven bag	White	PP	Linear cracks
	P46	Plastic bag	Blue	PE*	Corrosion pits
	P47	Plastic bag	White	LDPE	Corrosion pits
S16	P48	Plastic bag	White	HDPE	Flaking
	P49	Plastic bag	Black	HDPE	Rough surface
	P50	Packing bag	Translucent	LDPE	Crumples
	P51	Plastic bag	Translucent	PE*	Wrinkles
S17	P52	Plastic bag	Blue	LDPE	Corrosion pits
	P53	Packaging tape	Mustard	PP	Linear cracks
	P54	Packing bag	White	HDPE	Flakes
S18	P55	Plastic bag	White	HDPE	Adhering fibrous particles
	P56	Packing bag	Multicolor	HDPE	Wrinkles and scratch
	P57	Plastic bag	Translucent	LDPE	Corrosion pits

	P58	Packing bag	Translucent	LDPE	Grooves and fractures
	P59	Balloon	Multicolor	HDPE	Surface oxidation
	P60	Plastic bag	Translucent	PE*	Flaking
	P61	Packing bag	White	LDPE	Wrinkles and scratchs
	P62	Plastic bag	Yellow	PE*	Physical scratch
	P63	Plastic bag	Red	PE*	Smooth and physical scratch
	P64	Plastic bag	Translucent	LDPE	Wrinkles and cracks
	P65	Plastic bag	Translucent	HDPE	Flaking
	P66	Plastic bag	Black	LDPE	Rough surface
	P67	Plastic bag	Translucent	PE*	Wrinkles and cracks
	P68	Packing bag	Translucent	HDPE	Smooth, surface cracks
	P69	Plastic bag	Translucent	HDPE	Flaking
	P70	Packing	Blue	LDPE	Crumples and fragments
	P71	Plastic bag	Red	HDPE	Smooth
	P72	Plastic bag	Translucent	HDPE	Rough surface filamentous, cracking
	P73	Plastic bag	White	LDPE	Grooves
	P74	Balloon	Multicolor	PP	Severe surface cracking
	P75	Packing	Gray	PE*	Rough surface filamentous, cracking
	P76	Plastic bag	Translucent	LDPE	Wrinkles
	P77	Packing	Translucent	HDPE	Adhering fibrous particles
	P78	Plastic bag	Translucent	LDPE	Corrosion pits
S19	P79	Packing	White	PE*	Grooves
	P80	Plastic bag	Translucent	HDPE	Smooth, surface cracks
	P81	Plastic bag	Black	LDPE	Flaking
	P82	Plastic bag	Red	PE*	Grooves
	P83	Plastic bag	Translucent	LDPE	Corrosion pits
	P84	Plastic bag	Translucent	PE*	Wrinkles and scratchs
	P85	Packing bag	Multicolor	PP	Rough surface and physical scratch
	P86	Plastic bag	Black	PE*	Surface oxidation
	P87	Packing bag	Blue	PE*	Adhering fibrous particles
	P88	Plastic bag	Black	LDPE	Surface oxidation
	P89	Packing	Yellow	PE*	Grooves and scratches
	P90	Plastic bag	Translucent	PP	Rough surface
	P91	Plastic bag	Black	HDPE	Wrinkles and scratchs
	P92	Plastic bag	Translucent	HDPE	Uneven surface
S20	P93	Plastic bag	Black	LDPE	Corrosion pits
	P94	Packing	Translucent	PE*	Flaking
	P95	Packing	Translucent	HDPE	Surface oxidation
	P96	Plastic bag	Translucent	LDPE	Corrosion pits
	P97	Balloon	White	LDPE	Smooth and physical scratch
	P98	Plastic bag	Translucent	PE*	Grooves
S21	P99	Woven bag	White	PP	Surface cracking
	P100	Plastic bag	White	HDPE	Flaking
	P101	Packing bag	Silver	LDPE	Smooth, surface cracks
	P102	Plastic bag	Translucent	LDPE	Corrosion pits
S22	P103	Plastic bag	White	HDPE	Short rod-like, and worm-like pits

PE* refers to undistinguished PE due to strong fluorescence.

Table S-3 The measured results of corrosion pits through PiFM of PE samples.

Sample code	Thickness (μm)	Volume (μm^3/50×50 μm)	Density of pits (No./50×50 μm)	Depth of pits (μm/pit) (Mean±SD)	Area of pits (μm^2/pit) (Mean±SD)	Volume of pits (μm^3/pit) (Mean±SD)	Ratio of pit volumes[#] (%)
P11	24.976	62440	19.3	1.10±0.79	18.86±14.93	30.18±43.77	1.86
P12	21.304	53260	27.3	1.28±0.45	14.12±9.89	19.86±19.78	2.04
P18	23.734	59335	24.7	1.21±0.56	16.63±11.24	24.43±22.19	2.04
P19	25.848	64620	19.7	1.13±0.53	12.06±9.68	17.4±17.62	1.06
P20	26.369	65922.5	22	1.33±0.61	11.43±13.14	18.1±29.34	1.20
P27	26.913	67282.5	27.3	1.05±0.44	16.22±8.21	17.41±11.43	1.42
P39	28.467	71167.25	32.3	0.92±0.49	9.66±9.27	11.87±15.35	1.08
P40	13.236	33090	24.7	2.16±0.84	30.66±21.66	74.15±72.59	11.06
P46	14.303	35757.5	26.5	1.93±0.94	25.97±23.72	65.38±92.38	9.70
P47	14.925	37312.5	26	1.71±1.02	23.28±19.71	57.17±80.45	7.96
P52	18.717	46792.5	30.2	1.36±0.75	25.14±14	34.85±28.6	4.50
P57	16.196	40490	29.7	1.69±0.99	19.65±19.15	42.25±67.37	6.20
P78	15.803	39507.5	24.3	1.38±0.76	45.69±48.91	84.53±155.29	10.40
P83	14.528	36320	27.7	1.81±0.73	25.98±24.52	55.24±73.97	9.70
P93	19.804	49510	26.7	1.48±0.57	9.89±10.51	18.05±23.11	1.94
P96	15.223	38057.5	24.3	1.73±0.64	19.15±7.61	34.31±21.87	4.38
P102	13.724	34310	30.3	2.02±1.04	28.7±32.46	77.97±131.36	13.72
P103	21.102	52755	31.7	1.48±0.76	7.69±4.24	12.75±10.42	1.54

[#] Ratio of pit volumes = (Volume of pits×Density×2)/ Volume×100%
('×2' indicates that both sides of plastics in the deep sea were degraded simultaneously)

Supplementary Figures

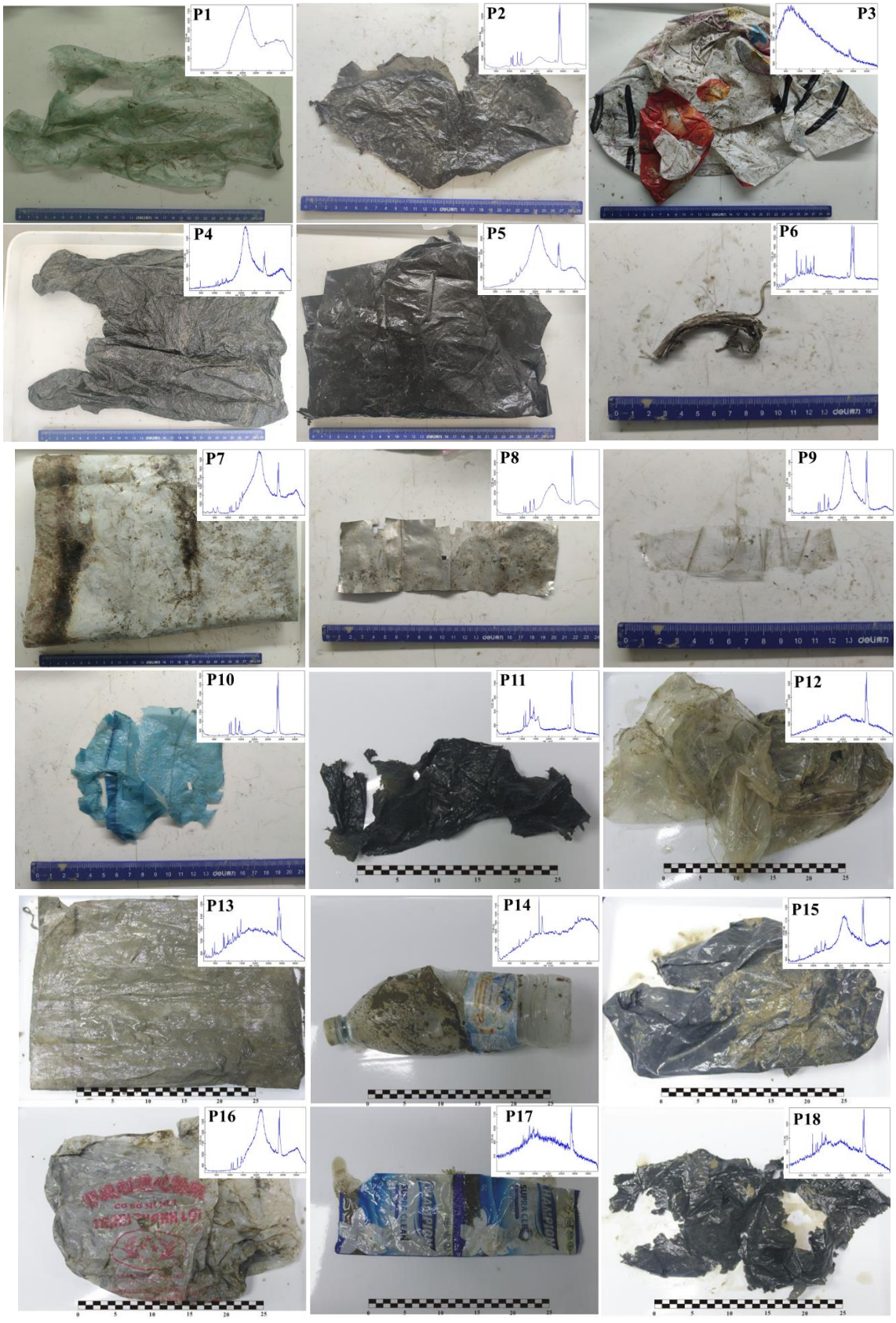

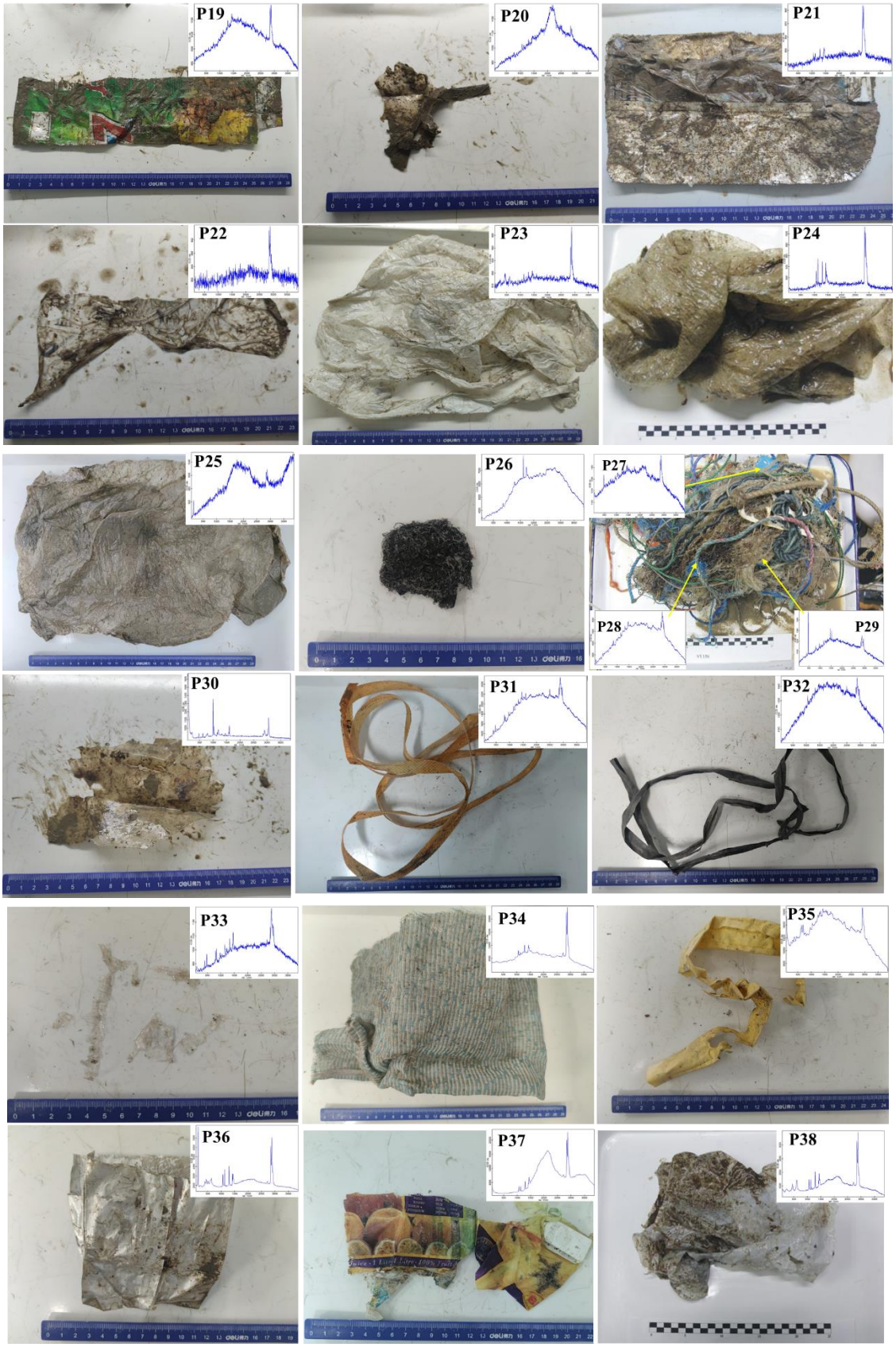
P19
P20
P21
P22
P23
P24
P25
P26
P27
P28
P29
P30
P31
P32
P33
P34
P35
P36
P37
P38

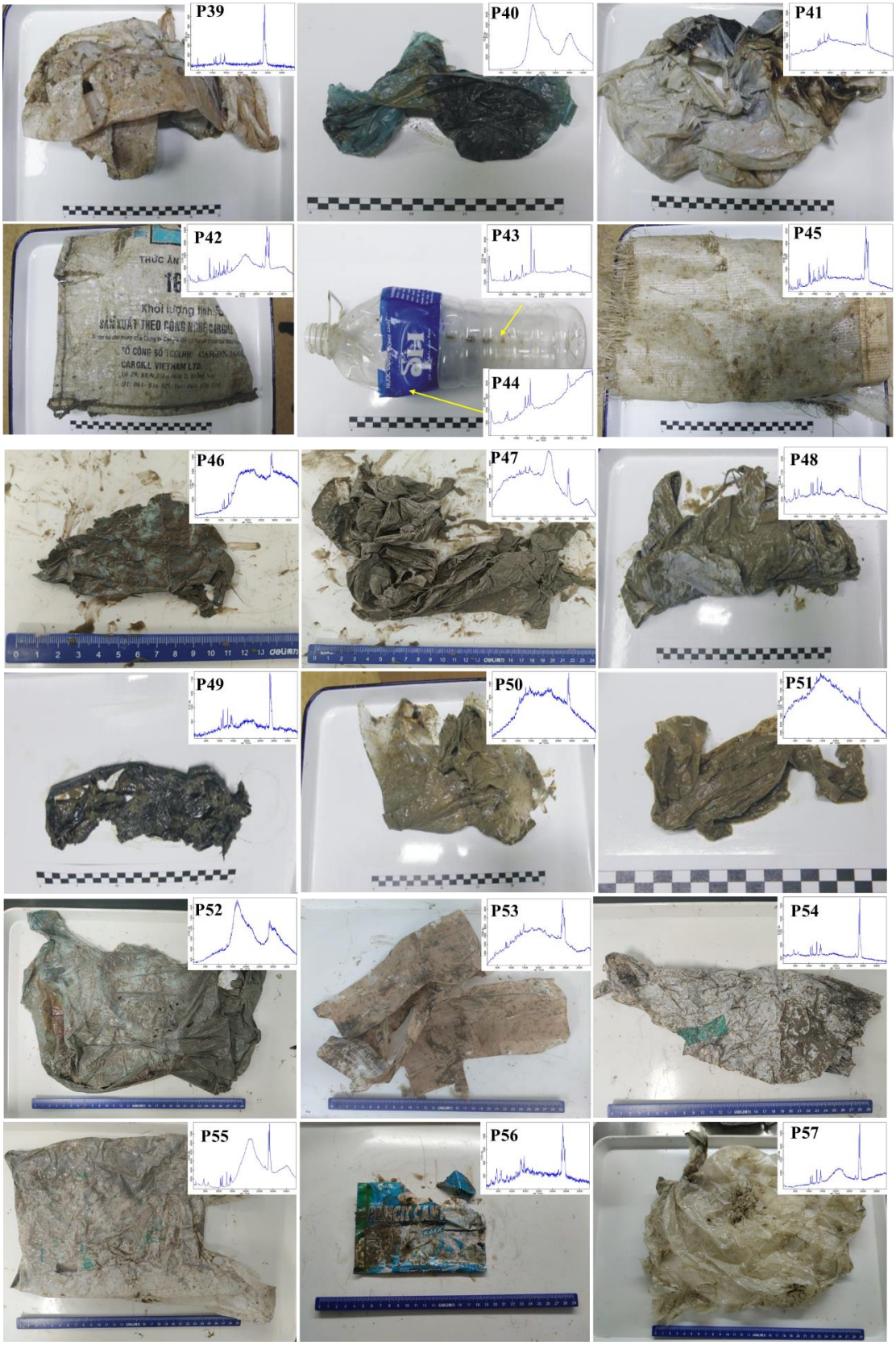
P39
P40
P41
P42
P43
P44
P45
P46
P47
P48
P49
P50
P51
P52
P53
P54
P55
P56
P57


P58
P59
P60
P61
P62
P63
P64
P65
P66
P67
P68
P69
P70
P71
P72

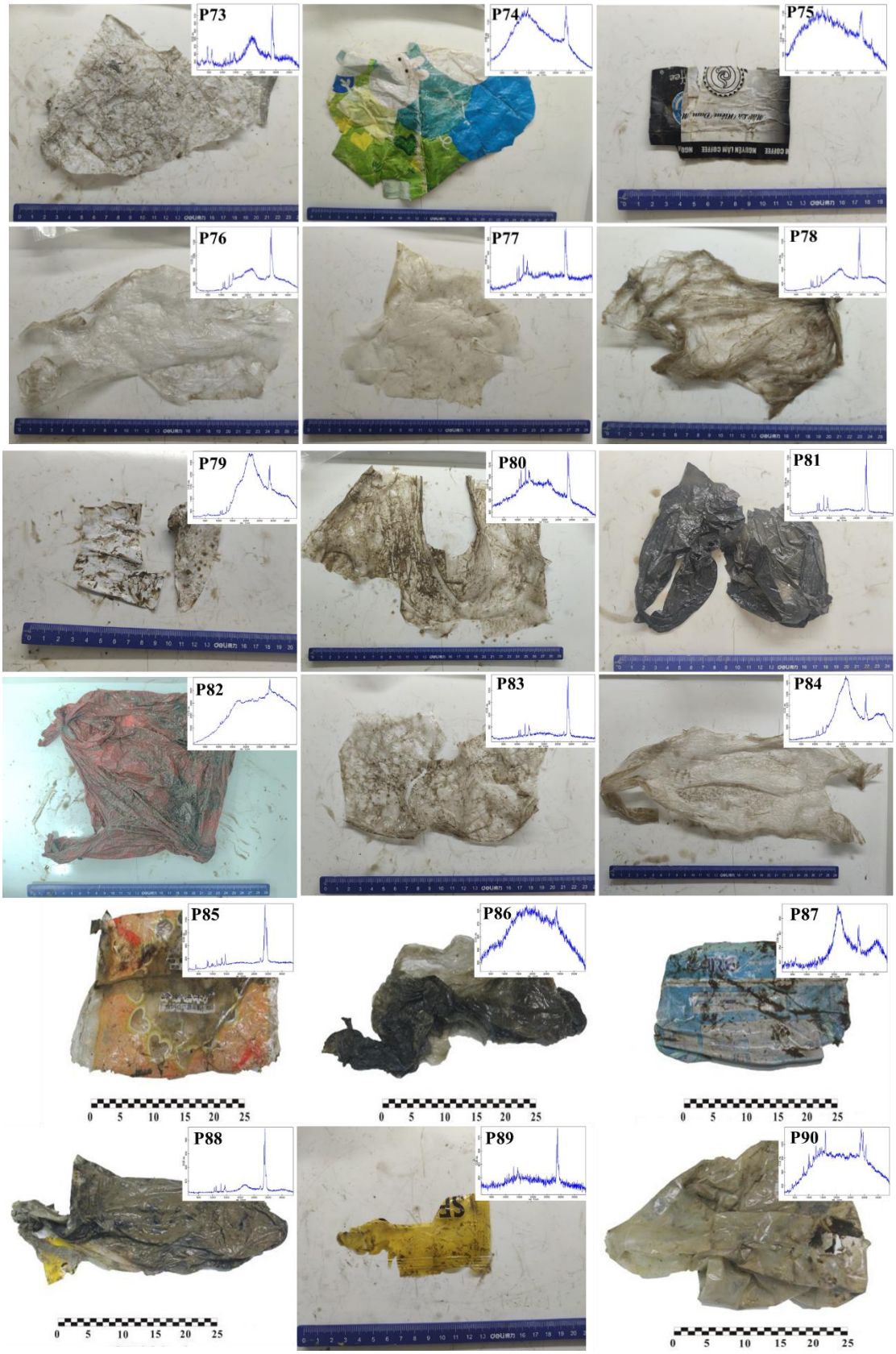
P73
P74
P75
P76
P77
P78
P79
P80
P81
P82
P83
P84
P85
P86
P87
P88
P89
P90
0 5 10 15 20 25

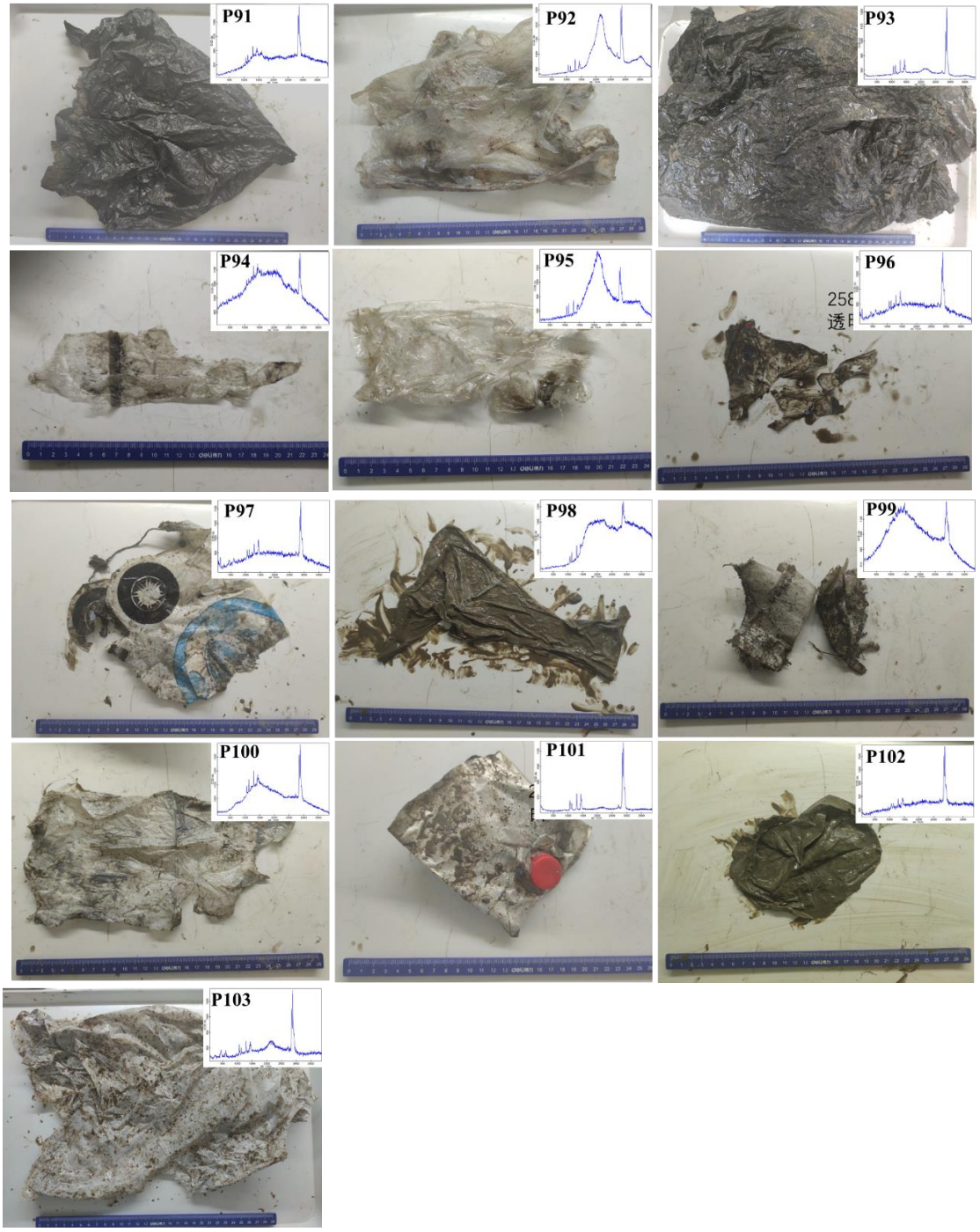

Figure S-1 Pictures of the plastic samples and corresponding Raman spectrum (inset).

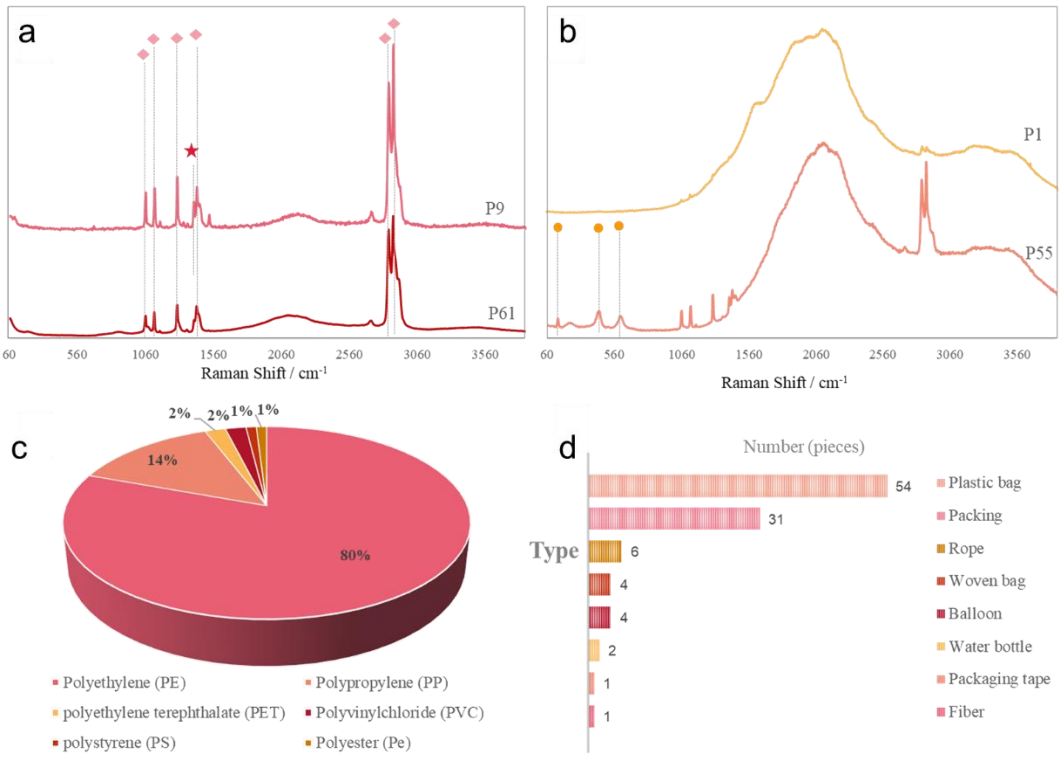

Figure S-2 Examples of FTIR spectrum of different PE samples **(a)** and **(b)** PE (pink rhombus from left to right: 1062, 1128,1295, 1440, 2849, and 2882 cm^{-1}; red pentagram: 1421 cm^{-1}; yellow circle from left to right: 141, 445 and 608 cm^{-1}); polymer composition **(c)** and usage type **(d)** distribution of plastics in deep seafloor of SCS.

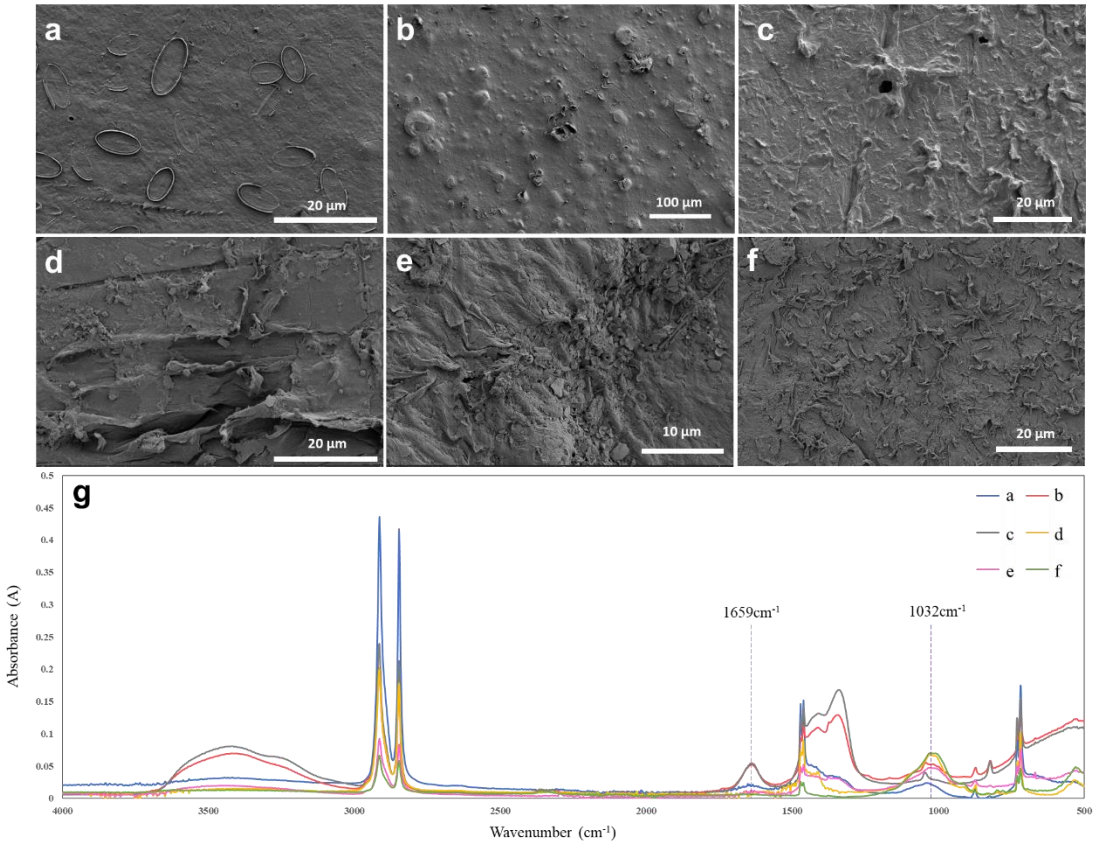

Figure S-3 Examples of SEM images and FTIR spectrum of different weathered PE samples. **(a)** some diatoms adhered to the smooth surface of P2. **(b)** uneven, hilly surface of P15 with numerous protrusions. **(c)** flakes, grooves and scratches on the surface of P16. **(d)** The irregular cracks caused by mechanical erosion on the surface of P47. **(e)** wrinkled surface of P89 **(f)** plenty of fibrous flakes attached to the surface of P54. **(g)** FTIR spectrum of the selected examples (a-e).

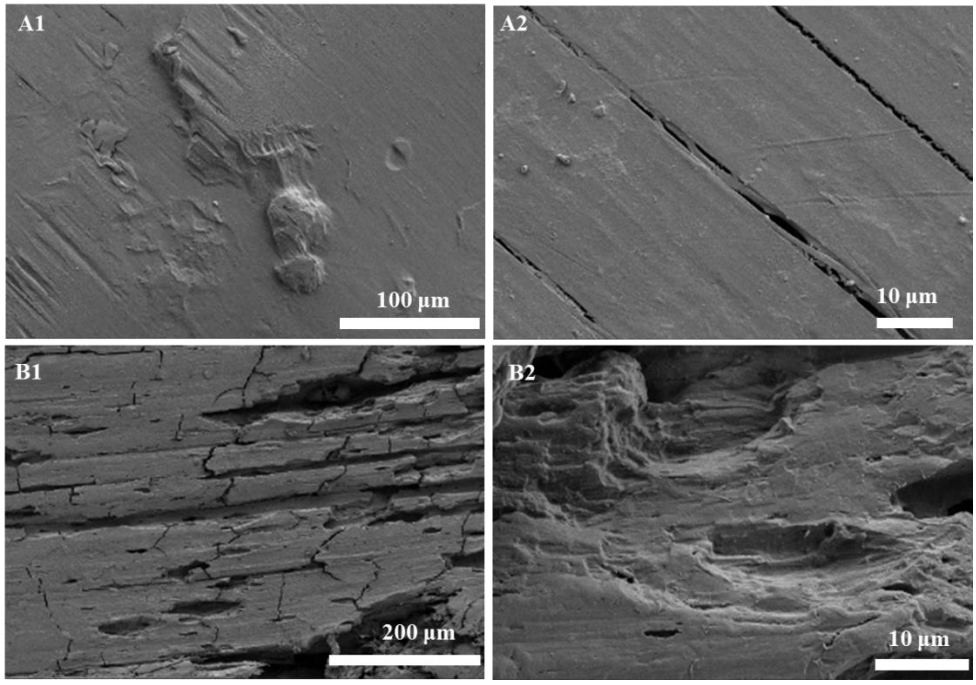

Figure S-4 Examples of SEM images and FTIR spectrum of different weathered PP samples. Each sample is displayed in two magnifications. **(a1, a2)** P29, **(b1, b2)** P33.

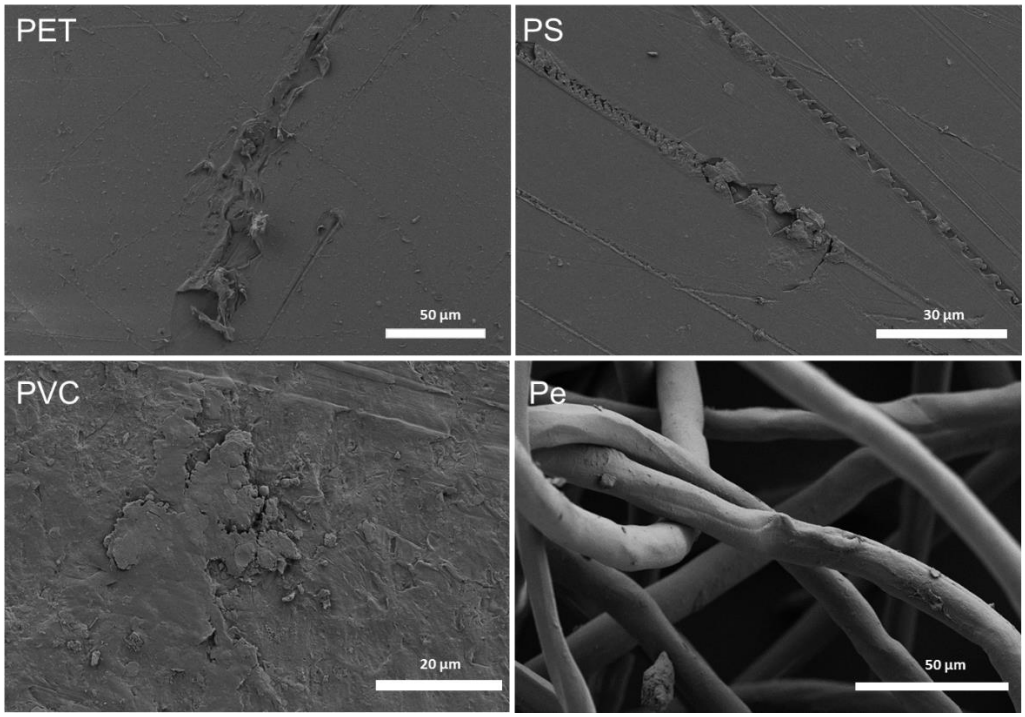

Figure S-5 SEM images of surface topography of PET, PS, PVC, and Pe collected from deep seafloor.

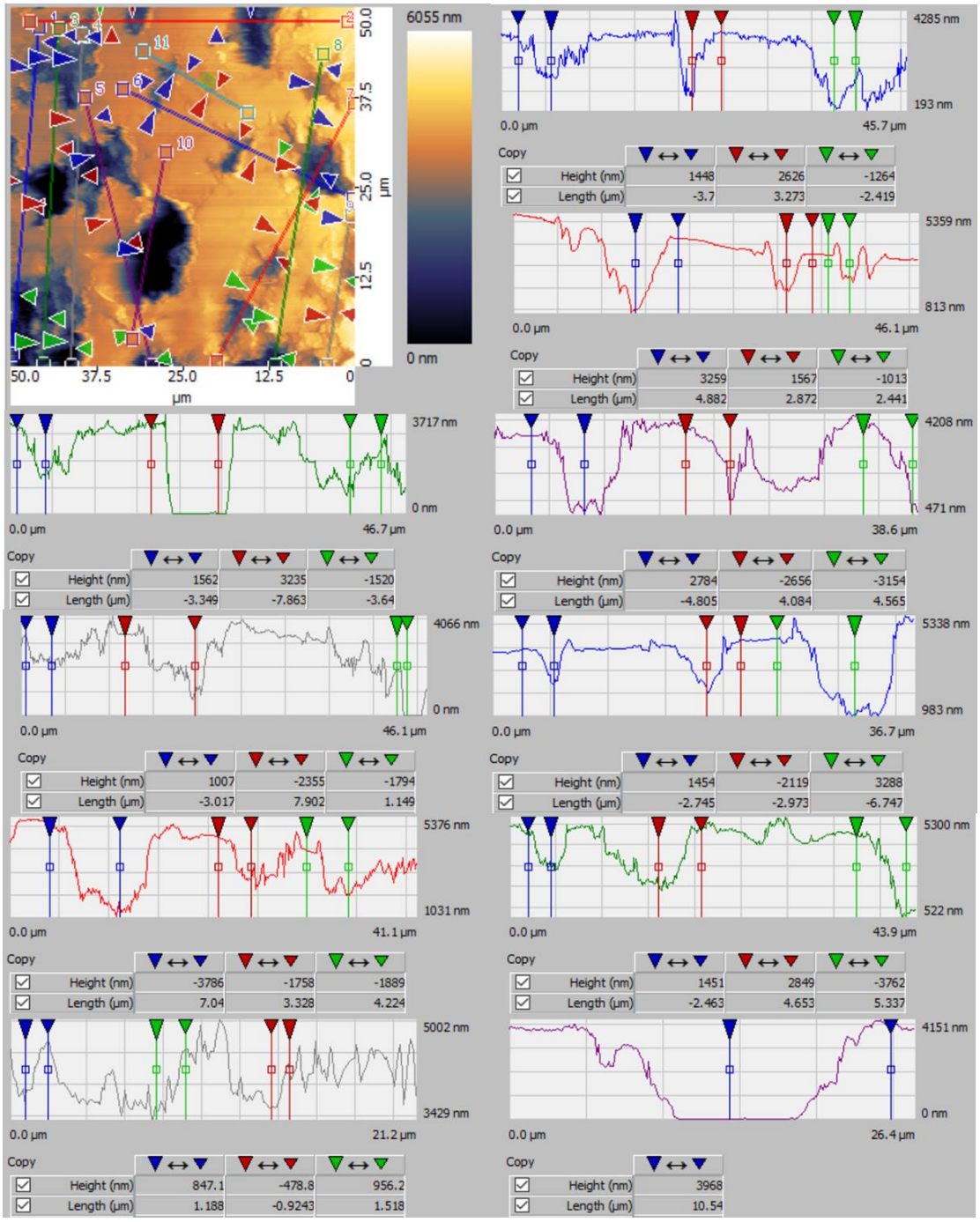

Figure S-6 PIFM images of P102 and the cross-sectional analysis along the line by SurfaceWorks (Height and Length are the vertical and horizontal distances between two cursors).

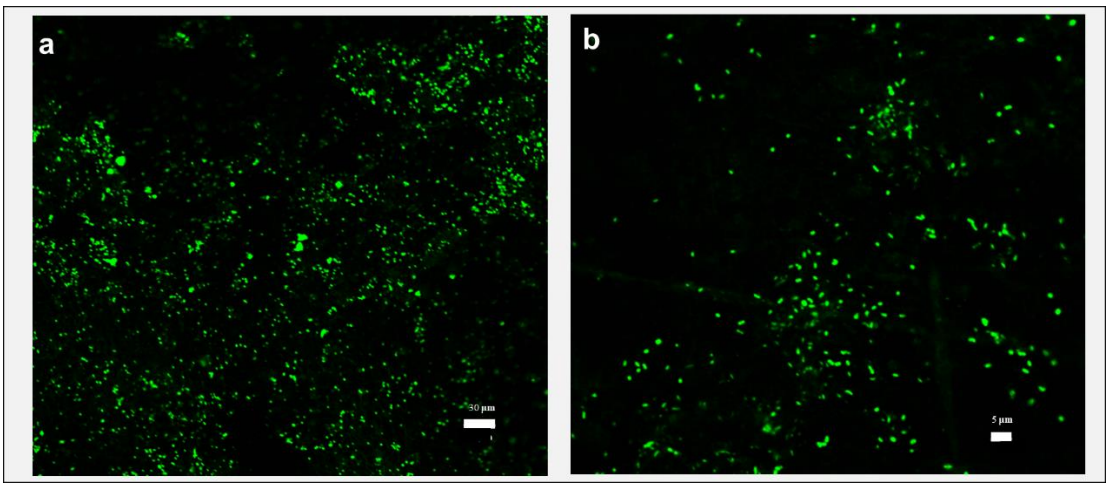

Figure S-7 **(a)** and **(b)** Images of SYBR green I stained surfaces of PE plastics.

Supplementary Information References

Briggs, C., Jones, M. (2005) SYBR Green I-induced fluorescence in cultured immune cells: a comparison with Acridine Orange. *Acta histochemica* 107, 301–312. https://doi.org/10.1016/j.acthis.2005.06.010

Käppler, A., Fischer, D., Oberbeckmann, S., Schernewski, G., Labrenz, M., Eichhorn, K.J., Voit, B. (2016) Analysis of environmental microplastics by vibrational microspectroscopy: FTIR, Raman or both? *Analytical and Bioanalytical Chemistry* 408, 8377–8391. https://doi.org/10.1007/s00216-016-9956-3

Lenz, R., Enders, K., Stedmon, C.A., Mackenzie, D.M., Nielsen, T.G. (2015) A critical assessment of visual identification of marine microplastic using Raman spectroscopy for analysis improvement. *Marine Pollution Bulletin* 100, 82–91. https://doi.org/10.1016/j.marpolbul.2015.09.026

Nauendorf, A., Krause, S., Bigalke, N. K., Gorb, E.V., Gorb, S. N., Haeckel, M., Wahl, M., Treude, T. (2016) Microbial colonization and degradation of polyethylene and biodegradable plastic bags in temperate fine-grained organic-rich marine sediments. *Marine Pollution Bulletin* 103, 168–178. https://doi.org/10.1016/j.marpolbul.2015.12.024

Sato, H., Shimoyama, M., Kamiya, T., Amari, T., Šašic, S., Ninomiya, T., Siesler, H.W., Ozaki, Y. (2002) Raman spectra of high-density, low-density, and linear low-density polyethylene pellets and prediction of their physical properties by multivariate data analysis. *Journal of Applied Polymer Science* 86, 443–448. https://doi.org/10.1002/app.10999